Available online at www.sciencedirect.com

SciVerse ScienceDirect

www.elsevier.com/locate/brainres

BRAIN RESEARCH

Research Report

Suppression of electrical synapses between retinal amacrine cells of goldfish by intracellular cyclic-AMP

*Soh Hidaka**

Department of Physiology, Fujita Health University School of Medicine, Toyoake, Aichi 470-1192, Japan

ARTICLE INFO

Article history:
Accepted 22 January 2012
Available online 28 January 2012

Keywords:
Retinal amacrine cell
Gap junction
Electrical synapse
Tracer coupling
Cyclic AMP
High voltage electron microscopy

ABSTRACT

Retinal amacrine cells of the same class in cyprinid fish are homotypically connected by gap junctions. The permeability of their gap junctions examined by the diffusion of Neurobiotin into neighboring amacrine cells under application of dopamine or cyclic nucleotides to elucidate whether electrical synapses between the cells are regulated by internal messengers. Neurobiotin injected intracellularly into amacrine cells in isolated retinas of goldfish, and passage currents through the electrical synapses investigated by dual whole-patch clamp recordings under similar application of their ligands. Control conditions led us to observe large passage currents between connected cells and adequate transjunctional conductance between the cells (2.02±0.82 nS). Experimental results show that high level of intracellular cyclic AMP within examined cells block transfer of Neurobiotin and suppress electrical synapses between the neighboring cells. Transjunctional conductance between examined cells reduced to 0.23 nS. However, dopamine, 8-bromo-cyclic AMP or high elevation of intracellular cyclic GMP leaves gap junction channels of the cells permeable to Neurobiotin as in the control level. Under application of dopamine (1.25±0.06 nS), 8-bromo-cyclic AMP (1.79±0.51 nS) or intracellular cyclic GMP (0.98±0.23 nS), the transjunctional conductance also remains as in the control level. These results demonstrate that channel opening of gap junctions between cyprinid retinal amacrine cells is regulated by high level of intracellular cyclic AMP.

1. Introduction

Gap junctions are intercellular membrane channels that subserve direct cell-to-cell communication for the exchange of ions and small molecules resulting in metabolic and electrical coupling of cells (Bennett et al., 1991). Individual intercellular channels are dodecameric structures consisting of two hexameric connexons (channel protein particles), provided by either of the two communicating cells. Gap junctions are made up of clusters that are aggregates of connexons. Each connexon is a hexameric structure composed of subunit proteins called connexins, each of which has four transmembrane domains. The connexins represent a family of proteins composed of a variety of members known to exist in mammalian tissue (Bruzzone et al., 1996; Goodenough et al., 1996; White and Paul, 1999).

In the vertebrate retina, electrophysiological measurements and microinjection of tracer molecules have revealed extensive gap-junctional communication among every class of adult neurons (Bloomfield and Völgyi, 2009; Hidaka et al., 1993, 2004, 2005; Naka and Christensen, 1981; Söhl et al., 2005; Vaney, 1991, 1994) and during neuronal development

* Fax: +81 562 93 2649.
E-mail address: shidaka@fujita-hu.ac.jp.

0006-8993/$ – see front matter © 2012 Elsevier B.V. All rights reserved.
doi:10.1016/j.brainres.2012.01.054

(Penn et al., 1994). The transmission of electrical signals via gap-junctional pathways influences the response properties and receptive-field organization of adult retinal neurons (Hidaka et al., 1993, 2004, 2005; Mastronarde, 1983, 1989; Meister et al., 1995; Poznanski and Umino, 1997; Umino et al., 1994). Although many factors modulate gap-junctional communication in brain and retinal neurons, little is known about the molecular structure of the connexin proteins mediating these effects. Recent molecular study of mammalian retinal neurons revealed that dopamine receptor-driven uncoupling of the cell network resulted from protein kinase A activation of protein phosphatase 2A and subsequent dephosphorylation of the neuronal gap junction connexin36 (Cx36) (Kothmann et al., 2009).

The amacrine cells in the vertebrate retina are laterally oriented interneurons that subserve synaptic interactions with bipolar cells, ganglion cells and other amacrine cells in the inner plexiform layer (IPL). It is generally accepted that amacrine cells can be classified into a number of functional classes, which reflect the morphological diversity of these cells (Masland, 2001). Amacrine cells make serial chemical synapses and gap junctional connections among these cells (Dowling, 1987). Amacrine cells are very likely to be inhibitory interneurons since these cells are labeled by anti-γ-aminobutyric acid (GABA) or anti-glycine antiserum (Yang et al., 1991). However, the functional roles of lateral connections between amacrine cells remain to be elucidated. Amacrine cells can be identified by their intracellularly recorded responses to light flashes. These cells have been demonstrated to summate response amplitudes beyond their dendritic field size in teleost retinas (Hidaka et al., 1993, 2005; Kaneko, 1973; Naka and Christensen, 1981). Our studies in retina from teleost fish: carp, goldfish, Japanese dace and black bass, have revealed that amacrine cells of the same class are homotypically interconnected by gap junctions with either tip-contact or cross-contact (Hidaka et al., 1993, 2005). The two patterns of tracer coupling between teleost amacrine cells are recognized. The cross-contact pattern is characterized by contact from the intermediate segment of one dendrite to that of another, as these dendrites cross over each other. This 'cross-contact' pattern occurred between amacrine cells with widely arborizing dendrites, and sustained photoresponses, and between amacrine cells with widely arborizing dendrites and transient photoresponses (Hidaka et al., 1993, 2005; Teranishi et al., 1987). The tip-contact pattern or tip-to-tip contact is characterized by contact between the tips of the dendrites of coupled cells. This 'tip-contact' pattern was observed between cells with narrow dendritic fields and transient photoresponses, as well as between cells with narrow dendritic fields with sustained photoresponses (Hidaka et al., 1993, 2005; Negishi and Teranishi, 1990, 1991; Teranishi et al., 1987). The amacrine cells with the tip-contact pattern or tip-to-tip gap junctional connection are called as "tip-contact amacrine cells". We have also identified three types of tip-contact amacrine cells in teleost retinas (Hidaka, 2008; Hidaka et al., 1993, 2005). These results suggest that the gap junctions between these neurons can extend their receptive fields and may enhance their inhibitory synaptic effects onto postsynaptic neurons in the IPL of the retina. Regulation of electrical synapses between amacrine cells of the same class appears to be a crucial function in retinal processing. If gap junction channels between homotypic amacrine cells are down-regulated by neuromodulators, inhibitory synaptic effects from these cells onto postsynaptic retinal neurons would be weak.

Kothmann et al. (2009) resolved a new mechanism in dopaminergic uncoupling effects in mammalian AII amacrine cells. A relationship between gap junction Cx36 phosphorylation and AII amacrine cell coupling strength was demonstrated. On the other hand, meclofenamic acid was recently introduced to block tracer coupling through gap junctions between specific neurons in the mammalian retina (Pan et al., 2007). These compounds appear to display many desirable properties as a gap junction antagonist. The suitability of meclofenamic acid in physiological studies is possible dissociation between tracer coupling and electrical coupling. Veruki and Hartveit (2009) demonstrated the block of electrical synapses evoked by meclofenamic acid between pairs of mammalian AII amacrine cells.

In the present study, I investigated whether gap junction channels between cyprinid retinal amacrine cells are modulated by internal messengers. The permeability of gap junctions between amacrine cells of the same class was examined by the diffusion of intracellularly injected Lucifer Yellow (LY) and biotinylated tracer, Neurobiotin, into neighboring cells under application of neuromodulators or internal messengers, since gap junctions are permeant to these molecules. The electrical synapses between homotypic amacrine cells were also investigated by dual whole-patch clamp methods under similar application of neuromodulators or internal messengers. Experimental results demonstrate that high level of intracellular cyclic AMP (cAMP) within these amacrine cells block transfer of LY and Neurobiotin to neighboring cells and suppress electrical synapses between these cells. However, dopamine or even high elevation of intracellular cyclic GMP (cGMP) leaves gap junction channels of these cells permeable to Neurobiotin into neighboring cells as in the control level. And electrical synapses between amacrine cells remain open under application of dopamine or intracellular cGMP.

2. Results

2.1. *Identification of cyprinid retinal amacrine cells*

Results were obtained from cells in retinas of goldfish. Among six physiologically identifiable classes of cyprinid amacrine cells (Hidaka et al., 1993, 2005), three types of tip-to-tip contact amacrine cells were examined for intracellular modulation of electrical synapses in the present study. Amacrine cells were identified with their light-evoked responses to spots of light and annuli illuminated on isolated retinas. When dark-adapted retinas were illuminated under relatively weak intensity at −3.0 log unit, amacrine cells were identified by their responses to flashes of light, transient ON–OFF, and sustained (Hidaka et al., 1993, 2005; Kaneko, 1970; Sakai and Naka, 1992; Teranishi et al., 1987). After light-evoked responses were recorded (not shown here, but see Fig. 1 of Hidaka et al., 2005), these cells were then labeled intracellularly to document their cellular morphology of amacrine cell types:

fusiform cell bodies extending their dendrites with interconnections at the tips (e.g. tip-to-tip contacts) in the IPL (Djupsund et al., 2003; Hidaka et al., 1993, 2005; Negishi, and Teranishi, 1990; Sakai et al., 1997; Teranishi and Negishi, 1991; Teranishi et al., 1987). Examined amacrine cells belonged to either of three amacrine cell classification types for such tip-contact cells (Hidaka et al., 1993, 2005). Fig. 1 shows flat view of three types of tip-to-tip contact amacrine cells under control conditions. These amacrine cells showed extensive Neurobiotin coupling with neighboring cells of the same morphological types. In Figs. 1D–F the vertical views of cells are shown. In Figs. 1A–C, individually recorded cells by microelectrode penetration of three amacrine cell types, and their hexagonally tracer-coupled neighbors are illustrated.

2.2. *Localization of gap junction connections at the dendritic tips*

To characterize structure of gap junctions between homologously connected tip-to-tip contact amacrine cells, dendritic tips between individual cells were examined by electron microscopy. The tip-to-tip connections are characterized by contact between the tips of the dendrites of Neurobiotin-coupled cells (Hidaka, 2008; Hidaka et al., 1993, 2005; Negishi and Teranishi, 1990, 1991; Teranishi et al., 1987).Ultrastructural analysis was performed by documenting tip-to-tip connections between cells with their light microscopic images (see Fig. 1). Fig. 2 shows anatomically identified gap junctions found between dendrites of a pair of interstitial amacrine cells (ISACs). High voltage electron microscopy of 5 μm thick sections revealed that junctional connections are laterally localized between Neurobiotin-labeled dendritic tips (Fig. 2A). The ultrathin sectioning analysis of the same cell of Neurobiotin labeling by conventional electron microscopy revealed anatomically identifiable gap junctions comprising of seven-layered components with close membrane apposition (Hidaka et al., 1989, 1993, 2004) are laterally localized between Neurobiotin-labeled dendritic tips (e.g. at the tip-contacts) (Fig. 2B). Their structural characteristics of gap junctions shown in Fig. 2B were confirmed with the fine structure of those between non-labeled dendrites found in the IPL (arrowheads, Fig. 2C). The area of close membrane apposition composing of seven-layered components (arrowheads, Fig. 2C) shows anatomically identifiable gap junction. The plasma membranes of the two dendritic processes came to within 1.5-2.0 nm of one another, but no closer, leaving a discernible gap between the dendrites. At tip-to-shank contacts, smaller gap junctions were also found.

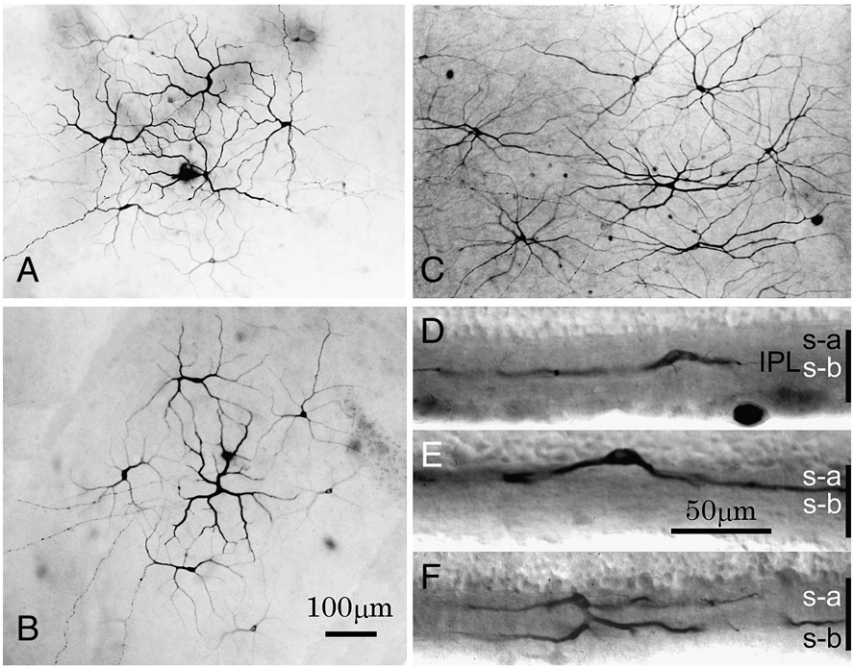

Fig. 1 – Cellular morphology and tracer coupling of cyprinid retinal amacrine cells. Intracellular recordings of flash-evoked responses from amacrine cells are shown in Fig. 1 of Hidaka et al. (2005). *A*, Cells generating sustained depolarizing responses are hexagonally connected at tip-to-tip contact (tip-contact) with neighbors of the same type, extending their dendrites only at the proximal part (sublamina b, s-b) of the inner plexiform layer (IPL) (*D*). These cells are interstitial amacrine cells. *B*, Cells generating sustained-type responses with transient depolarizations at the cessation of the light stimuli are also hexagonally coupled at tip-contact with neighbors of the same type, extending their dendrites only at the distal part (sublamina a, s-a) of the IPL (*E*). These cells are normally placed monostratified tip-contact amacrine cells. *C*, Cells generating transient depolarizations at the ON or OFF set of light stimuli are hexagonally tracer-coupled at dendritic tips with neighbors of the same type (*F*), extending their dendrites at both sublaminas (the distal (s-a) and proximal (s-b) layers) of the IPL. These cells are transient ON-OFF bistratified tip-contact amacrine cells. Vertical bars in the right of *D–F* denote the thickness of the IPL. Scale bars: 100 μm for *A–C*. 50 μm for *D–F*.

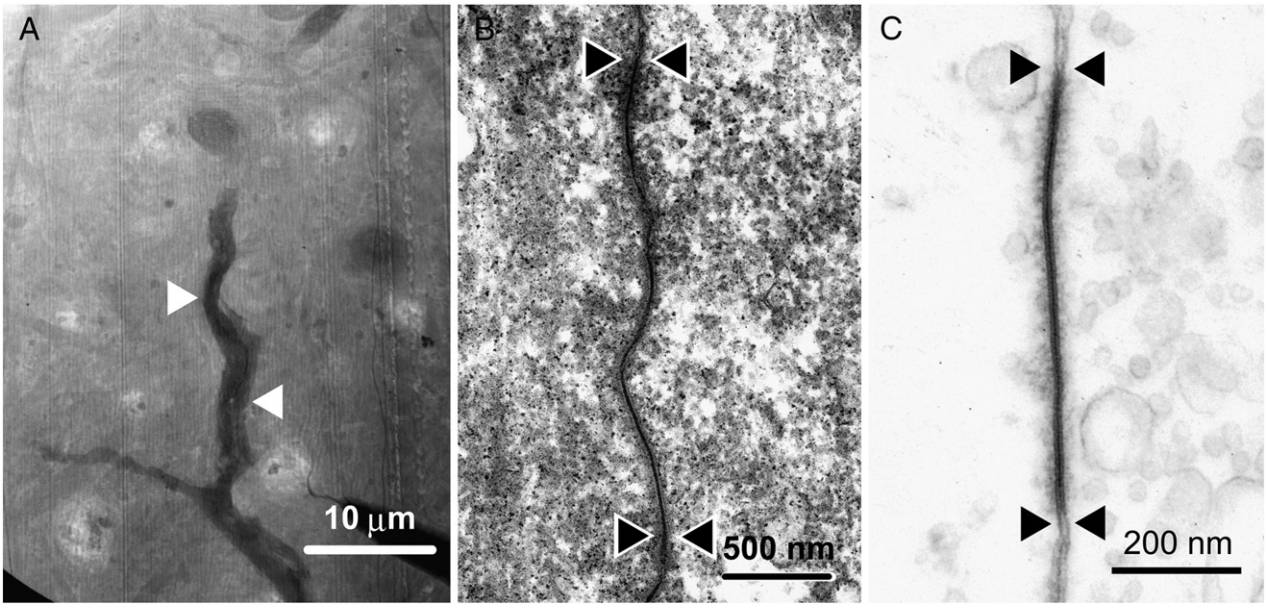

Fig. 2 – Ultrastructure of gap junctions in dendrodendritic tip-to-tip contacts between Neurobiotin-coupled cyprinid retinal amacrine cells. *A*, An electron micrograph of a dendrodendritic tip-to-tip connection by high voltage electron microscopy of interstitial amacrine cells generating sustained depolarizing responses. The specimen was observed at 1000 kV in a tangential 5-μm section in thickness. The direct junctional contact occurs between the tips of peripheral dendrites from Neurobiotin-coupled interstitial amacrine cells. Note the close apposition of the labeled dendrites of the two contacting cells as demarcated by *white arrowheads*. *B*, A gap junction formed between the tips of Neurobiotin-labeled peripheral dendrites (*between arrowheads*) from the tracer-coupled interstitial amacrine cells of the same cells shown in A by conventional electron microscopy of an ultrathin section at 75 kV. *C*, Conventional electron micrograph showing the fine structure of a gap junction (*between arrowheads*) between cells found in the inner plexiform layer of an ultrathin section at 75 kV. Plasma membranes of the two non-labeled dendrites are closely apposed with a narrow central gap, about 2.0 nm wide, between the outer leaflets of the apposed unit membranes. Scale bars: 10 μm for *A–B* and 500 nm for *C*.

Recently, connexins immunocytochemically have localized gap junctions between fish photoreceptor cells and bipolar cells (Li et al., 2009). Cx35 localizes gap junctions between fish photoreceptor cells, whereas Cx36 localizes gap junctions between mammalian AII amacrine cells and α-retinal ganglion cells (Hidaka et al., 2004). The antibodies against neural Cx35 or 36, Cx26, Cx32 or Cx43, however, failed to stain gap junctions between goldfish amacrine cells. It remains elusive what connexin types are localized in gap junctions between teleost amacrine cells.

2.3. *GABA involvement in cyprinid tip-to-tip contact amacrine cells*

To provide descriptive characterization of cellular properties of tip-to-tip contact amacrine cells, the content of their neurotransmitters was examined by specific antibodies against certain neurotransmitters. Fig. 3 shows GABA immunoreactivity in vertical cryosections of the retina. ISACs are GABA-immunopositive in addition to H1 cone horizontal cells (somata by H1 and axons by Hax) (Hashimoto et al., 1976; Kaneko, 1970; Marc et al., 1978; Stell et al., 1975) and somata of conventional amacrine cells localized in the inner most row of the inner nuclear layer (INL) (Fig. 3A). Immunolabeled interstitial amacrine cells (arrowhead) could be identified with their characteristic large soma within IPL, although the IPL displayed a dense immunoreactive plexus (Fig. 3A).

To demonstrate GABA contents in the normally placed monostratified amacrine cells by anti-GABA antibody, Lucifer yellow-filled (and also Neurobiotin-filling) cells, after recording of their light-evoked responses, were cryosectioned serially. Sections were double-labeled with avidin-rhodamine and a FITC-conjugation following incubation with the anti-GABA antibody for biocytin and GABA-immunoreactivity localization. Figs. 3B–C shows biocytin localization in the normally placed monostratified cell (red in Fig. 3B) extending their dendrites in the distal layer of the IPL and GABA localization within their soma (green in Fig. 3C, indicated by arrowheads). Transient ON–OFF bistratified tip-to-tip contact amacrine cells are also GABA-immunopositive (not illustrated). These results demonstrate that three types of tip-to-tip contact amacrine cells may use GABA as their neurotransmitters.

2.4. *Effects of intracellular cyclic nucleotides on gap junction permeability between cyprinid amacrine cells*

As shown in control condition (Fig. 1), individual tip-to-tip contact amacrine cells of the same morphological type show extensive Neurobiotin coupling. Effects of intracellular cyclic nucleotides, cAMP and cGMP, on gap junction permeability between goldfish amacrine cells were examined. When multiple chemical substances involved at the tips of sharp glass microelectrodes were, at the same concentration, ejected by passing the polarized currents in the time duration, the

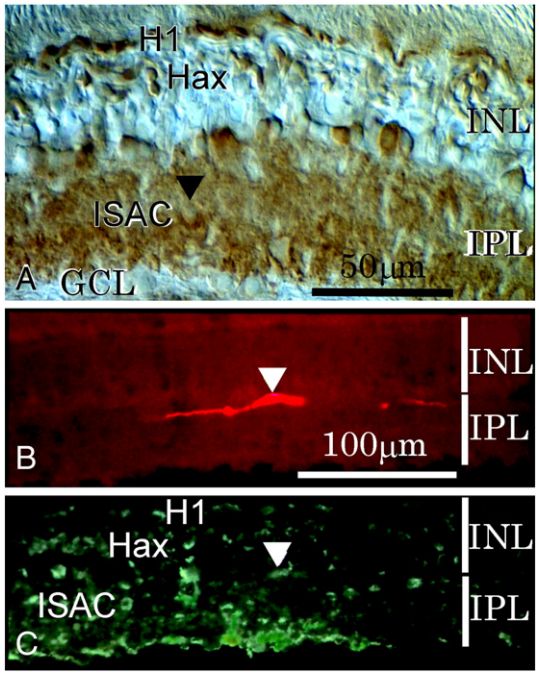

Fig. 3 – GABA immunoreactivity in cyprinid retinal amacrine cells. A, Detection of GABA in a vertical cryosection section of the retina by anti-GABA serum. GABA immunoreactivity was observed in somata of fish cone horizontal cells (H1), their axon terminals (Hax), conventional amacrine cells in the innermost low of the inner nuclear layer (INL) and interstitial amacrine cells (ISAC) within GABA immunopositive dendritic plexus of the IPL. B, Rhodamine labeling of normally placed monostratified amacrine cells generating sustained-type responses with transient depolarizations at the cessation of the light stimuli in a vertical section. C, GABA localization in the normally placed amacrine cell in the section shown in B. The amacrine cell showed FITC labeling by GABA immunoreactivity after the section was processed with anti-GABA serum and FITC conjugate secondary antiserum. Note that FITC immunofluorescence was also observed in H1, their Hax, conventional amacrine cells in the INL and ISAC in the IPL. Scale bars: 50 μm for A and 100 μm for B and C.

currents can equilibrate both influx of Neurobiotin and cyclic nucleotides from the glass electrode into the cell in the electrophoresis (Hidaka, 2008; Hidaka et al., 1993, 2004, 2005). The intracellular cyclic nucleotides at the concentration of 300 mM were used, since Neurobiotin was ejected at 6% volume. cAMP of 300 mM concentration corresponds to 6% volume. When 300 mM cAMP in addition to 3% LY and 6% Neurobiotin in glass microelectrodes, cAMP was simultaneously injected into individual amacrine cells together with Neurobiotin by passing positive currents, high elevation of intracellular cAMP led to no diffusion of LY or Neurobiotin from the recorded cells into neighboring cells (see Figs. 4 and 5). In the case of transient ON–OFF bistratified cells, LY (not shown) and Neurobiotin (Fig. 4B) remained only in the injected cells. For depolarizing interstitial amacrine cells, LY (not shown) and Neurobiotin (Fig. 5B) resulted in staining of only the injected cell. These results demonstrate that high dose of intracellular cAMP completely blocked transfer of LY and Neurobiotin to neighboring cells of the same morphological type.

When 8-bromo-cyclic AMP (8-br-cAMP) (2 mM), a membrane permeable cAMP, was perfused in extracellular bath solution, while intracellularly injecting Neurobiotin into the transient ON-OFF amacrine cells, extensive Neurobiotin coupling between cells of the same morphological type, as seen in controlled condition was seen. After superfusion of retina with dopamine (100 μM), intracellularly injected Neurobiotin into the transient ON–OFF cells or depolarizing interstitial amacrine cells (Fig. 5A) resulted in strong transfer of Neurobiotin into many neighboring cells of the same morphological type as seen in control condition. It is known that dopamine activates D_1 receptor, thereby elevating concentration of intracellular cAMP to activate protein kinase A (Neve et al., 2004). Recent reports in mammalian AII amacrine cells described stimulation of D_1 receptor by dopamine resulting in protein kinase A activation of protein phosphatase 2A to induce uncoupling between cells (Kothmann et al., 2009). However, results of this study suggest that small elevation of intracellular cAMP concentration within fish tip-contact amacrine cells does not suppress permeability of their gap junction channels.

When 3% Lucifer yellow, 6% Neurobiotin and 300 mM cGMP in sharp microelectrodes, cGMP was simultaneously injected into the transient ON-OFF bistratified cells, together with Neurobiotin by passing positive currents, the transient ON-OFF cells showed Neurobiotin coupling in several neighboring cells of the same morphological type, as seen in control condition (Fig. 4A). This observation shows that even high elevation of intracellular cGMP concentration does not block permeability of gap junction channels between transient ON-OFF amacrine cells. For normally placed monostratified cells, exogenously applied dopamine (100 μM) or intracellularly injected cGMP never blocked permeability of gap junction channels between these cells.

2.5. *Effects of electrical synapses between goldfish amacrine cells by intracellular cyclic nucleotides*

Dual whole-cell patch-clamp recordings in control condition measure electrical junction conductance (Gj) in pairs of interstitial amacrine cells in retinal slice preparation. The junction conductance was estimated with both cells in voltage clamp by applying a series of test voltages to the presynaptic cell and recording the generated currents in both the pre- and the postsynaptic cell (Fig. 6). The relationship between junction voltage (Vj) and junction current (Ij) was linear (Fig. 6A), when corrected for nonzero series resistance and finite membrane input resistance. This result indicates that Gj was independent of Vj over the range of test voltages (±30 mV). The junctional conductance was then measured as the slope of a straight line fitted to the I–V relation (1.32 nS, Fig. 6B). The Gj for a cell pair was calculated as the slope conductance determined from each direction of coupling and plotted for both directions of coupling for each cell pair (Fig. 6C). This result shows that the electrical junction conductance of interstitial amacrine cells in control condition was symmetric without rectification. The mean Gj was 2.02±0.82 nS (n=9 cell pairs; range 1.10–3.64 nS).

When patch pipettes with 5 mM cAMP were applied to pair of interstitial amacrine cells in dual whole-cell recordings, junction currents (I_2) were dramatically decreased (Fig. 7B).

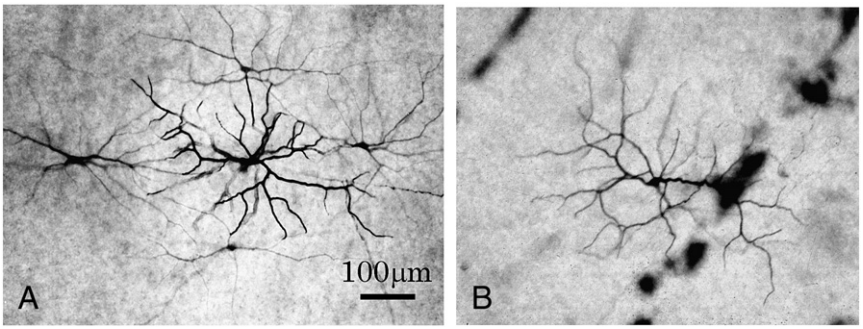

Fig. 4 – Intracellular cyclic AMP (cAMP) blocks permeability of gap junction channels between cyprinid transient ON-OFF bistratified tip-contact amacrine cells. In the control condition, injection of Neurobiotin into transient ON–OFF amacrine cells (Fig. 1C) revealed strong diffusion of the tracer into many neighboring amacrine cells of the same type. *A*, Intracellular injection of cyclic GMP (cGMP) (300 mM) left diffusion of Neurobiotin into neighboring cells as in the control level. *B*, Intracellular injection of cAMP (300 mM) blocked transfer of Neurobiotin into neighboring cells. Scale bars: 100 μm for *A* and *B*.

Gj decreased to 0.23 nS ± 0.05 nS (n = 6 cell pairs) in the presence of intracellular cAMP (Fig. 7C), and Gj decreased to 0.97 ± 0.23 nS (n = 4 cell pairs; range, 0.78–1.25 nS), when 5 mM cGMP in patch pipettes (Fig. 8). When 8-br-cAMP (2 mM) was perfused in extracellular bath solution, mean Gj between pairs of interstitial amacrine cells in dual whole-cell recordings remained in the control level (1.79 ± 0.51 nS, n = 5 cell pairs; range 1.10–2.55 nS). After superfusion of retina with dopamine (100 μM), mean Gj between pairs of interstitial amacrine cells was 1.25 ± 0.06 nS (n = 4 cell pairs; range 1.17–1.32 nS). Electrical junction conductance of goldfish interstitial amacrine cells against applied ligands is summarized in Fig. 8. These results demonstrate that a high dose of intracellular cAMP in interstitial amacrine cells can block electrical synapses between them. Small elevation of intracellular cAMP concentration within these amacrine cells by membrane-permeable 8-br-cAMP or application of dopamine, however, does not decrease electrical coupling between them. Even high elevation of intracellular cGMP concentration does not appear to affect electrical coupling between them, although Gj decreased to the statistically dominated level by 5 mM cGMP in patch pipettes (single asterisk in Fig. 8). Microinjection of 5 mM cGMP into tip-contact amacrine cells remained in strong Neurobiotin coupling pattern as seen in the control level, showing negative effects.

3. Discussion

The present study has measured regulation of permeability of intracellular markers and electrical junctional conductance of gap junctions between cyprinid tip-to-tip contact amacrine cells. This refines our knowledge about electrical synapses of homologous (i.e. connected with cells of the same morphological type) retinal neurons. Although knowledge of regulation of gap junctions between retinal amacrine cells has been determined in several different ways (Hampson et al., 1992; Kothmann et al., 2009), this is the first report based on direct simultaneous measurement of regulation of electrical synapses between amacrine cells by dual whole-cell patch clamp recordings. This approach has served to clarify effects of intracellular cAMP on gap junctions, including the confirmation of block of gap junction permeability by cAMP and a more quantitative assessment about almost complete suppression of electrical synapses by high level of intracellular cAMP but not high concentration of intracellular cGMP,

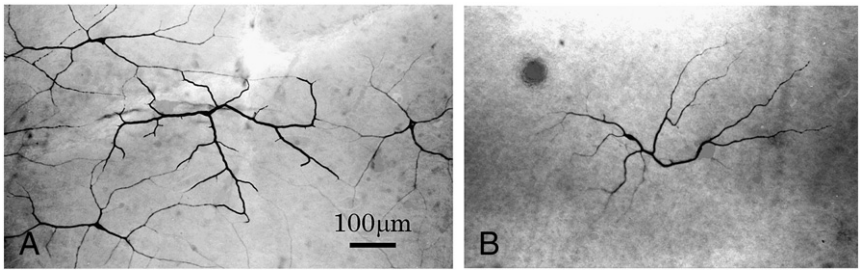

Fig. 5 – Intracellular cAMP suppresses permeability of gap junction channels between cyprinid sustained monostratified tip-contact amacrine cells. In the control condition, interstitial amacrine cells (ISACs) generating sustained depolarizing responses (Fig. 1A) and normally placed amacrine cells producing sustained hyperpolarizing responses (Fig. 1B) showed strong Neurobiotin coupling into many neighboring amacrine cells of the same type. *A*, Dopamine (100 μM) did not block permeability of gap junctions between sustained hyperpolarizing normally placed amacrine cells. *B*, Intracellular injection of cAMP (300 mM) into ISACs suppressed transfer of Neurobiotin into neighboring cells. Scale bars: 100 μm for *A* and *B*.

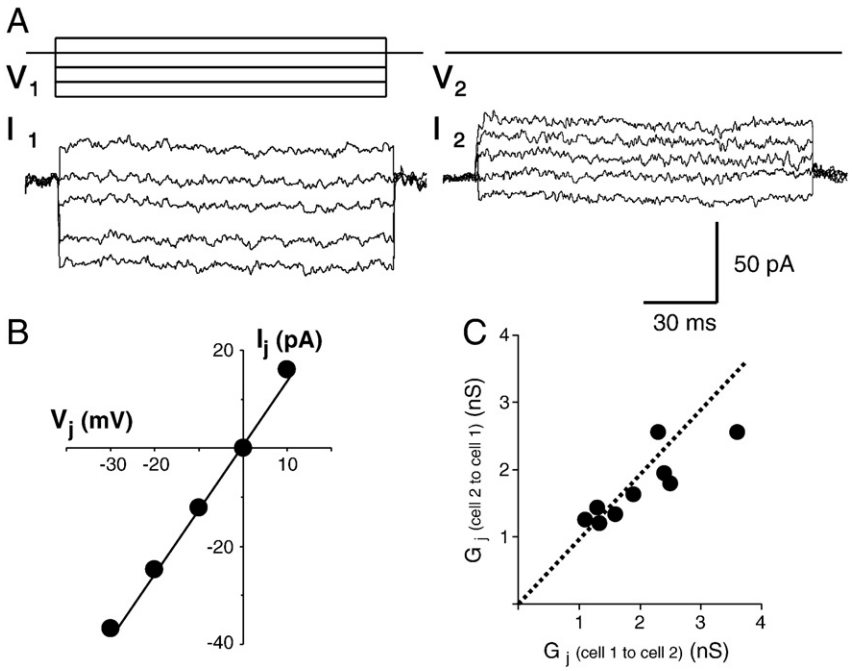

Fig. 6 – Measurement of electrical junction conductance (Gj) between cyprinid ISACs. *A*, With both cells in whole-cell voltage clamp (V1 and V2), voltage steps (–90 to –50 mV, 10 mV increments) from holding potential of –60 mV were applied to one cell (V_1) and current responses were recorded in both cells (I_1 and I_2). *B*, Current–voltage relationship between the junctional current (Ij) and the junctional voltage (Vj) shown in A. The plotted data are fit with a straight line which slope shows Gj (1.32 nS). *C*, Summary of Gj. Comparison of Gj in each direction shows nonrectifying electrical synapses, when electrical coupling in the same cell pair was examined in both directions [e.g. Gj (cell 1 to cell 2) for cell 1 presynaptic, and Gj (cell 2 to cell 1) for cell 2 presynaptic]. The dashed line indicates the values expected when Gj is the same in both directions for pairs of ISACs.

extracellularly applied membrane permeable analog, 8-bromo-cAMP or dopamine.

3.1. *Large increase of the level of intracellular cAMP blocks the permeability of the gap junctions and electrical synapses between teleost amacrine cells*

The present study showed that exogenous dopamine did not reduce the tracer coupling between cyprinid amacrine cells, nor suppress the electrical junction conductance of electrical synapses between the cells. Even high dose of exogenous dopamine (100 μM) did not reduce the tracer coupling or the electrical synapses. D_1 receptors are classically regarded as having micromolar sensitivity to dopamine, whereas D_2 receptors are regarded as having nanomolar sensitivity (Kebabian and Calne, 1979). Previous dose–response curves for the effect of dopamine on cAMP production indicated that 100 nM dopamine produced no significant increase in cAMP (Hampson et al., 1992; Van Buskirk and Dowling, 1981; Watling et al., 1979), whereas a saturating response required at least 100 μM dopamine (Schorderet, 1989). In teleost horizontal cells shown in previous studies (DeVries and Schwartz, 1989; Lasater, 1987; Lasater and Dowling, 1985; Piccolino et al., 1984; Teranishi et al., 1983, 1984; Van Buskirk and Dowling, 1981; Watling et al., 1979), 100 μM dopamine could induce significant uncoupling when they appear to increase the levels of intracellular cAMP.

In the present study, significant uncoupling between cyprinid tip-contact amacrine cells occurred by increased levels of cAMP with incubation of several hours after 300 mM (or 6%) cAMP was intracellularly injected through recording microelectrodes. For measurement of electrical synapses by dual whole-cell patch clamp methods, several minutes after patching cells of a pair allowed permitting the cell cytosol to equilibrate with the pipette solution. When 5 mM cAMP was added in patch pipettes, significant amount of intracellular cAMP (introduced by patch pipettes) would diffuse to the dendritic tips localizing gap junctions of interstitial amacrine cells, if the cAMP is in part degraded by possible phosphodiesterases in several minutes. Highly increased levels of intracellular cAMP need to suppress the tracer coupling or the junctional current of goldfish tip-contact amacrine cells, because exogenous dopamine and a membrane permeable 8-br-cAMP did not reduce the tracer coupling or the junctional current. Goldfish tip-contact amacrine cells may lack dopamine receptors elevating intracellular cAMP or be insensitive to nanomolar level of cAMP. It is possible that cAMP would be directly associated with gap junctions of goldfish cells. I conclude that suppression of electrical synapses between these cells with dual patch clamp measurement is physiologically significant due to the occurrence by increased levels of intracellular cAMP.

Kothmann et al. (2009) showed that the tracer coupling did not show complete block in dopaminergic uncoupling effects in rabbit AII amacrine cells. They showed a relationship

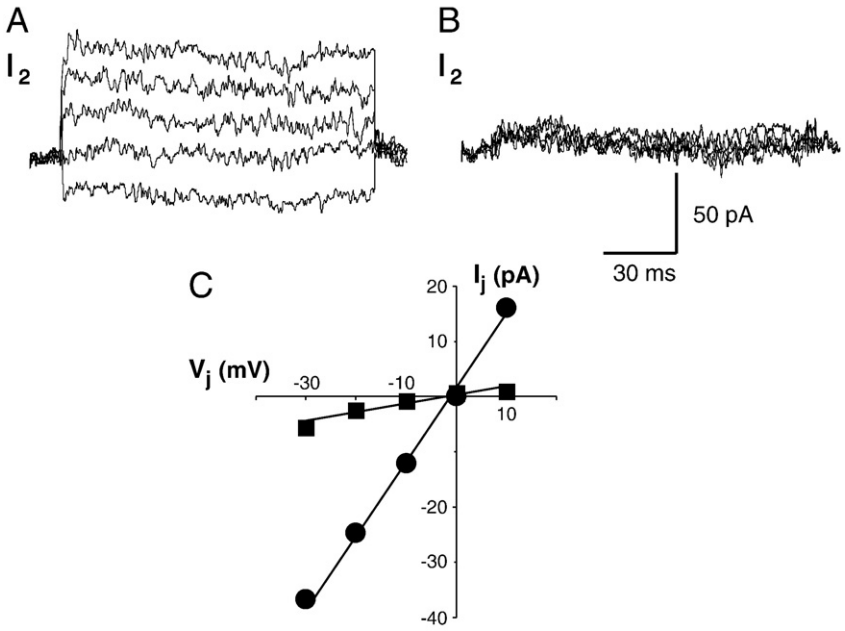

Fig. 7 – Intracellular cAMP reduces electrical junction conductance between cyprinid ISACs. A, In a control condition, junctional currents (I_2) appeared in one cell when voltage steps (–90 to –50 mV, 10 mV increments) from holding potential of –60 mV with both cells in whole-cell voltage clamp were applied to the other cell. Average electrical junction conductance (Gj) between ISACs for the control condition was 2.02 ± 0.82 nS (n = 9 pairs). *B*, Involvement of 5 mM cAMP in pipette decreased junctional currents (I_2). *C*, Comparison of current–voltage relationship between the junctional current and the junctional voltage shown for the control condition and involvement of cAMP. From the plotted data for the control condition (circles) and involvement of cAMP (squares), individual Gj was calculated by the slopes for straight lines fit with the data, 1.32 nS for the control condition and 0.23 nS for involvement of cAMP, respectively.

between Cx36 phosphorylation and AII amacrine cell coupling strength. Dopamine receptor-driven uncoupling of the AII network resulted from protein kinase A activation of protein phosphatase 2A and subsequent dephosphorylation of Cx36. The present study of the teleost tip-to-tip contact amacrine cells clearly induced complete block of the tracer coupling by the intracellularly raised level of cAMP. These results suggest that production level of intracellular cAMP by exogenous dopamine does not induce complete block of the tracer coupling between rabbit AII amacrine cells via protein kinase A activation. It is necessary for high dose of intracellular cAMP to completely block the tracer coupling between neighboring cells of rabbit AII cells. Intracellular perfusion by 5 mM cAMP in patch pipettes under dual whole-cell patch clamp recordings revealed significant block of electrical synapses between goldfish amacrine cells occurred by highly raised levels of intracellular cAMP. Thus high dose of intracellular cAMP significantly affects opening of gap junction channels between cyprinid tip-contact amacrine cells.

Mechanisms are yet to be fully understood gap junction uncoupling between the teleost amacrine cells occurred by highly raised levels of intracellular cAMP. It is known that raised level of cAMP activates a cAMP-dependent protein kinase, probably leading to phosphorylation of the gap junction protein in teleost fish horizontal cells (DeVries and Schwartz, 1989; Lasater, 1987; Lasater and Dowling, 1985; McMahon et al., 1989; Piccolino et al., 1984; Teranishi et al., 1983, 1984). On the other hand, Kothmann et al. (2009) recently resolved a new mechanism in dopaminergic uncoupling effects in Cx36-expressing mammalian AII amacrine cells. Dopamine receptor-driven uncoupling of the mammalian AII network resulted from protein kinase A activation of protein phosphatase 2A and subsequent dephosphorylation of gap junction protein Cx36. No Cx36 expressed in cyprinid amacrine cells. To date the connexin expressed in goldfish amacrine cells is unknown. In addition, the gap junction coupling between the horizontal cells is sensitive to pH changes (DeVries and Schwartz, 1989; Negishi et al., 1985) as well as the raised level of cGMP (DeVries and Schwartz, 1989). The present study showed the gap junction coupling between the teleost amacrine cells does not appear to be sensitive to the highly raised level of cGMP, although the effect and sensitivity to intracellular pH changes were not examined. The mechanism underlying gap junction uncoupling of the teleost amacrine cells is substantially different from that established for teleost horizontal cells and mammalian AII amacrine cells to exogenous dopamine and intracellular rising of cGMP.

3.2. *Functional consequences of intracellular modulation of electrical synapses between amacrine cells*

One fundamental function of the retina is to adapt to fluctuating background illumination. The general role of amacrine cells in the retinal neuron network remains a mystery. For example, the role of amacrine cells in the formation of a concentric receptive field remains unknown. The lack of knowledge

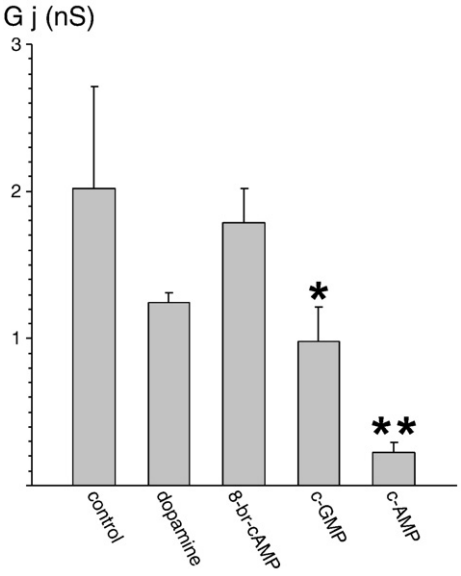

Fig. 8 – Summary of electrical junction conductance (Gj) between cyprinid ISACs when examined ligands were applied. Comparison of Gj under control conditions and applied ligands: dopamine (100 μM), 8-bromo-cyclic AMP (8-br-cAMP, 2 mM), cyclic GMP (cGMP, 5 mM) and cyclic AMP (cAMP, 5 mM). Data are shown as mean ± SEM. Statistical significance was evaluated by Student's *t* test. Gj under application of cyclic GMP shows $^{*}p<0.05$ to that of control conditions. Under application of cyclic AMP, $^{**}p<0.001$ was demonstrated, compared with control condition.

on the amacrine cell's function is partly due to the fact that, except for the directionally selective mammalian amacrine cells (Fried and Masland, 2007; Masland, 2005; Poznanski, 2005, 2010a, 2010b; Taylor and Vaney, 2003; Vaney and Taylor, 2002), the functional relationship between amacrine cells and ganglion cells remains unresolved. Moreover, the mode of signal transmission from amacrine cells to ganglion cells remains unknown in most retinas so far studied. One possible exception, however, is the role of electrical coupling between retinal neurons. Electrical coupling between photoreceptor cells increases the signal-to-noise ratio of their response to light (Baylor et al., 1974), and these functional properties appear to agree with electrical synapses of mammalian AII amacrine cells (Dunn et al., 2006; Vardi and Smith, 1996). Dopaminergic modulation of coupling strength between AII amacrine cells serves to optimize signal-to-noise ratio for prevailing background illumination and is one mechanism the retina uses to accomplish luminance adaptation (Bloomfield and Völgyi, 2004).

Teranishi et al. (1987) showed that interstitial and normally placed amacrine cells in carp retina were not dye-coupled when Lucifer yellow was injected into them. The amacrine cells producing a transient ON-OFF response had a bilayered dendritic field, which was confined to a narrow stratum in the IPL (Teranishi et al., 1987). The morphology of some amacrine cells reported by Negishi and Teranishi (1990) that produced a transient ON-OFF depolarizing response is very similar to that of sustained amacrine cells (N cells) in gourami retina (Sakai et al., 1997). Djamgoz et al. (1989) also reported a class of amacrine cells with similar morphology in the goldfish retina, and a flash stimulus generated a sustained response from these cells. These amacrine cells had a monolayered dendritic field within a narrow stratum of the IPL. By injection of biocytin or Neurobiotin, Hidaka et al. (1993, 2005) revealed that all examined amacrine cells that belong to certain similar types were tracer coupled in Japanese dace retina. Teranishi and Negishi (1994) also observed that the majority of amacrine cells of certain similar types were tracer coupled, using Neurobiotin. Gap junctions are present between amacrine cells of certain similar types in fish retinas (Hidaka et al., 1993, 2005; Marc et al., 1988). These observations on the tracer coupling of amacrine cells in various classes of retina cannot be dismissed simply as artifacts (Vaney, 1994); there must be reasons that explain why the majority of amacrine cells are extensively tracer coupled as we have shown in our papers (Hidaka et al., 1993, 2005). Thus the demonstration that the cyprinid tip-to-tip contact amacrine cells show extensive tracer coupling, together with the electron microscopic evidence that these neurons are connected by gap junctions, securely establishes that the individual populations of tip-to-tip contact cells form a coupled syncytium.

It is unknown neuromodulators, inducing highly rise of intracellular cAMP production that block gap junction channels of tip-to-tip contact amacrine cells. It is not possible that conventional physiological conditions induce highly raise of intracellular cAMP level to block of electrical coupling between the amacrine cells. The present study has shown that intracellular cAMP uncouples the tip-to-tip contact amacrine cells. If we accept that intracellular cAMP is raised tonically in certain conditions, then the findings from the present study suggest that intracellular cAMP may uncouple the retinal circuit associated with the amacrine cells in the inner retina. This would preserve the spatial acuity of the teleost photoreceptor circuit by preventing signal flow from teleost bipolar cells through the electrically coupled amacrine cell network. Under mesopic conditions, the sustained depolarizing responses of bipolar cells are barely apparent in tip-to-tip contact amacrine cell networks, whereas under scotopic conditions, the transient depolarizing responses of the tip-to-tip contact amacrine cells are reflected in the light-evoked response of teleost rod-dominant ON-center bipolar cells (Dacheux and Raviola, 1986; Kaneko, 1970, 1973; Kolb and Nelsen, 1983; Nelson, 1982; Umino et al., 1994). Such circuit switching would be compatible with cAMP's other possible diverse functions, all of which is associated with the transition from scotopic to photopic vision.

4. Conclusion

The purpose of this study was to elucidate regulation mechanisms of gap junctions and electrical synapses between goldfish retinal amacrine cells by internal messengers. This article is the first report based on direct simultaneous measurement of regulation of electrical synapses between amacrine cells by dual whole-cell patch clamp recordings. The present study has measured regulation of gap junction permeability of intracellular markers, LY and Neurobiotin, and gap junction

conductance between cyprinid fish tip-to-tip contact amacrine cells. This approach has served to clarify effects of intracellular cAMP on gap junctions, including the confirmation of block of gap junction permeability by cAMP and a more quantitative assessment about almost complete suppression of electrical synapses by high level of intracellular cAMP but not high concentration of intracellular cGMP, membrane permeable analog, 8-br-cAMP or dopamine. The present study suggests that novel mechanisms, apart from activation of protein kinases by cyclic nucleotides, are present in retinal amacrine cells of teleost and possibly other species as are.

5. Experimental procedure

5.1. *Animal use*

Experiments were carried out with goldfish (*Carassius auratus*). Animal use was in accordance with the legislation by the Physiological Society of Japan regulating the use of animals in research. Fish were maintained in an aquarium under natural daylight conditions until use. The animals were dark-adapted for 1–2 h before operation to facilitate separation of the retina from the pigment epithelium. The fish were deeply anesthetized with Tricaine (MS222; # A-5040, Sigma, St. Louis, MO) added to the water (0.01–0.02% solution), before operation for removal of eyeballs from animal bodies. Retinas were isolated under dim red light, and then placed on filter membrane paper (catalog # AAWG01300; Millipore, Bedford, MA) in photoreceptor cell-side up, using slight suction to remove the vitreous humor and make it adhere.

5.2. *Intracellular labeling and dye transfer measurement*

For microelectrode labeling of retinal amacrine cells, the intracellular injection technique of dyes via glass micropipettes was utilized (Hidaka et al., 1993, 2005) after analysis of their light-evoked responses (see below). Micropipettes were pulled from borosilicate glass capillaries (outer diameter, 1.0 mm; inner diameter, 0.58 mm, Clark Electromedical Instruments, Pangbourne, England) with a vertical pipette puller (Model 700 C, David Kopf Instruments, Tutunga, CA), filled at their tips with 3% Lucifer Yellow (Aldrich, Milwaukee, WI) and 6% biotinylated tracer: biocytin (Sigma) or Neurobiotin (Vector Laboratories, Burlingame, CA), dissolved in 0.5 M LiCl and 0.05 M Tris buffer (pH 7.6), and then backfilled with 3 M potassium acetate. Lucifer Yellow (LY) was used for identification of success of intracellular impalement into amacrine cells by micropipettes. Final DC resistances of these microelectrodes ranged from 350 to 450 Mohm. Individual amacrine cell in the retina was impaled with an electrode connected with a high-impedance amplifier (M-707, World Precision Instruments, Sarasota, Florida, or MEZ-8301, Nihon Kohden, Tokyo, Japan). LY and the biotinylated tracer were then injected into the cell, by passing polarized currents of ±1 nA, duration of 500 ms, at 1 Hz for 2 to 15 min.

The Neurobiotin-injected retinas were fixed in fixative containing 4% paraformaldehyde and 0.15 M NaCl in 0.1 M phosphate buffer saline (PBS), pH 7.4, for 2 h at room temperature. Following fluorescent microscopical confirmation of single-cell LY labeling of individual injected cells to exclude specimens of double (or multiple) microelectrode penetration or LY leakage into neighboring cells under a blue excitation (Nikon), the localization of Neurobiotin was visualized by incubation with a solution of either avidin–biotin–HRP complex (ABC; Elite kit; Vector Laboratories) in PBS (pH 7.5) or horseradish peroxidase streptavidin (Vector Laboratories) in PBS (pH 7.8), and followed by the reaction with diaminobenzidine (DAB; Dozin, Tokyo, Japan). Tracer coupling and dendrodendritic connections between amacrine cells were microscopically examined and photographed in black-white negative (Kodak T-MAX 400) or color positive films (Fujichrome PROVIA 400 F). Images were taken into a PC-type computer using Adobe Photoshop application program, equipped with a 35 mm film scanner (LS-1000; Nikon). Neurobiotin-labeled specimens were also utilized for electron microscopic analysis (see below).

5.3. *Intracellular recordings of light-evoked responses*

Intracellular recordings were made from retinal amacrine ce–s, using methods described elsewhere previously (Chino and Hashimoto, 1986; Hidaka, 2008; Hidaka et al., 1993, 2005; Shimoda et al., 1992; Umino et al., 1994). The retina was illuminated with light signals from two photostimulators. Light stimuli were produced by a computer-controlled system, using a 2500-W Xenon arc lamp through neutral density filters, interference filters (half-band width < 20 nm) and a variable field aperture mounted on a micrometer drive and an electromechanical shutter. All stimuli were presented in flashes of 250-ms duration at 2.0-s intervals. The intensity of the stimulus was 0.145 mW/cm^2 at 0.0 log unit when light passing through 550-nm interference filter was measured with a spectrophotometer (model 470D Radio Meter, Sanso Co., Tokyo, Japan) The retina was illuminated from the photoreceptor side. The stimuli were imposed on a diffuse white background light (intensity 10^{-7} W/cm^2 at 550 nm) illuminating the whole retina. After identification of the light-evoked responses of an individual cell, the cell was sequentially injected with LY, the biotinylated tracer and intracellular cyclic nucleotide, if involved (see below), by passing the polarized currents.

5.4. *Examination of the effects by intracellular cyclic nucleotides*

For control condition, and perfusion with dopamine or 8-bromo-cyclic AMP (Sigma), the tips of glass microelectrodes were filled with LY and either biocytin or Neurobiotin, dissolved in LiCl-Tris buffer. To examine the effects of intracellular cyclic nucleotides on the permeability of gap junctions between retinal amacrine cells, the tips of microelectrodes were involved with cyclic nucleotide (cAMP or cGMP) (Sigma), together with LY and the biotinylated tracer. The intracellular cyclic nucleotides at the concentration of 300 mM were used, since the biotinylated tracer was ejected at 6% volume. cAMP of 300 mM concentration corresponds to 6% volume. When multiple substances involved at the tips of microelectrodes were, at the same concentration, ejected by passing the polarized currents in the time duration, the currents can equilibrate both influx of the biotinylated tracer and cAMP from the glass electrode into the cell in the electrophoresis.

5.5. *Dual whole-cell patch-clamp recordings of electrical synapses*

The electrical coupling between retinal amacrine cells described below was measured from pairs of cells in retinal slice preparations. Electrophysiological characterization of electrical synapses between amacrine cells was performed by dual whole-cell recordings using patch pipettes filled with an intracellular solution (see below) involving 0.5% Neurobiotin and 0.1% LY. For whole-cell recordings of these cells, the visually controlled intracellular recording technique via glass micropipettes under the fixed-stage microscope (Tauchi and Masland, 1984) was utilized. LY was used for identification of success of intracellular recordings into neurons by patch pipettes. For patch-clamp recordings from amacrine cells, the tissue was transferred to fish Ringer solution (see below) (which is continuously bubbled with O_2), placed in a superfusion chamber with ganglion cell-side up, and maintained at room temperature. The perfusion chamber was mounted on the stage of a fixed-stage upright light microscope (E-600FN type, Nikon, Tokyo, Japan), equipped with a patch-slice micro-incubator (Harvard, Holliston, MA, USA). The tissue was perfused at 1 ml/min with fish Ringer solution, bubbled with O_2. The tissue was viewed through a 40×/0.80NA, water immersion, long-working-distance objective (Nikon). Cell bodies of amacrine cells were identified by the size (more than 15 μm in diameter) and their characteristic nuclei under Nomarski differential interference illumination, localized in the IPL (Hidaka, 2008; Hidaka et al., 1993, 2005).

Recordings were made from these cells *in situ* to identify amacrine cells by the characteristic morphology of their somata and dendritic extension. In the experiments, the fish Ringer solution (the extracellular solution) bathing the retinas contained (in mM): 145 NaCl, 5 KCl, 2.5 $CaCl_2$, 10 HEPES, 10 glucose (320–330 mosmol/kg), and continuously bubbled with O_2 at room temperature. Chemicals were added to the external solution. The concentration of the chemicals was as follows (in μM): 30 3-(2-carboxypiperazin-4-yl)-propanephosphonic acid (CPP), 10 6-cyanol-7-nitroquinoxaline-2,3-dione (CNQX), 10 bicuculine, 1 strychnine, 2500 $CoCl_2$ (all Sigma), 1 tetrodotoxin (TTX; Sankyo, Tokyo, Japan).

Simultaneous dual whole-cell recordings were performed in ruptured-patch mode (Hidaka and Ishida, 1998; Hidaka et al., 2004, 2005; Sakmann and Neher, 1995), using dual Axopatch 200B amplifiers (Axon Instruments, Foster city, CA). Pipettes were pulled with the P-97 model pipette puller (Sutter Instruments, Novato, CA) from borosilicate glass capillaries (outer diameter, 1.5 mm; inner diameter, 0.86 mm, Sutter Instruments) to tip resistances of 3.5–5 Mohm. Pipette (intracellular) solution consisted of (in mM): 145 K-gluconate, 4 NaCl, 0.5 $CaCl_2$, 2 $MgCl_2$, 10 1,2-bis(2-aminophenoxy)ethane-N,N,N′, N′-tetraacetic acid (BAPTA), 10 HEPES, 5 Mg-ATP, 0.8 Na_2GTP. LY was added (1–5 μg/ml) to the internal solution, and the pH of this solution was adjusted to 7.5 with potassium hydroxide solution (total K^+ concentration was 145 mM). Osmolarity was adjusted to 310–320 mosmol/kg with sucrose. To examine the effects of intracellular cyclic nucleotides on the electrical synapses between amacrine cells, the microelectrodes were involved with 5 mM cAMP or cGMP (Sigma). The concentration of cyclic nucleotides effective to electrical synapses between amacrine cells was experimentally determined. When the internal solution involves cyclic nucleotides, the pH of the solution was also adjusted to 7.5 with potassium hydroxide solution (total K^+ concentration, 145 mM). Data are presented as mean ± SEM. Statistical significance was evaluated by Student's *t* test.

Closely located large cell bodies of more than 15 μm in diameter localized within the IPL were first approached by dual patch electrodes under Nomarski differential contrast images of the brightfield illumination. I targeted two large cell bodies about 100–200 μm apart, because they could probably be selected for interstitial amacrine cells (Djamgoz et al., 1989, 1990; Hidaka et al., 1993; Teranishi and Negishi, 1991; Teranishi et al., 1987; Wagner and Wagner, 1988) (see Results). These cells were sequentially patched using LY-filled pipettes. After the first cell was patched and series resistance of the cell was compensated, it took at least two minutes to patch the other cell of a pair. This time allowed permitting the cell cytosol to equilibrate with the pipette solution. Then the second cell was patched and series resistance was also compensated. When individual dendrites of these cells were filled with the dye under fluorescent observation, the presence of dendritic contacts could be identified. Depolarizing amacrine cells of the same morphological type expanded their dendrites in the proximal part (sublamina b) of the IPL (Famiglietti et al., 1977): i.e. interstitial amacrine cells of the same physiological type were connected with each other at their dendrites (see Results). After I established the whole-cell mode, cells were generally held at a membrane potential of −60 mV. The holding potentials were corrected for liquid junction potentials. Depolarizing and hyperpolarizing current pulses were applied to one of the potentially coupled amacrine cells. Voltage responses recorded in current-clamp mode from the other cell indicated electrical coupling between these neurons. The coupling coefficient between two cells was determined as the ratio of the voltage response in cell 2 divided by the voltage response in cell 1 under steady-state conditions. The fast current-clamp feedback circuitry of the Axopatch 200B was used in all current-clamp recordings. Current protocols and off-line analysis were performed with the pCLAMP 9 system (Axon Instruments). The voltage monitor output of the patch-clamp amplifier was analog-filtered with a Bessel filter that built-in to the Axopatch 200B (corner frequency = 1 kHz) and digitally sampled at twice the filter frequency (or faster). Series resistance typically measured less than 15 Mohm (range of values measured at the beginning of current measurements from individual cells: 7–14 Mohm). Cells with series resistance above 17 Mohm were excluded from analysis.

5.6. *Immunocytochemical analysis of GABA localization and connexin expression*

Following electrophysiological identification of amacrine cells (see above), the retinas containing Neurobiotin-labeled cells were processed for two step fixation to examine involvement of γ-aminobutyric acid (GABA) in the cells. First, the retinas were fixed in a mixture of 4% paraformaldehyde and 1% glutaraldehyde in 0.1 M PBS, pH 7.5, for 30 min at room temperature, and then 4% paraformaldehyde in 0.1 M PBS, pH10.4, for overnight at 4 °C. After washing in PBS, specimens containing Neurobiotin-labeled amacrine cells were incubated in avidin-

rhodamine (Vector Lab., Burlingame, CA) in PBS, diluted with 1: 200, for 2 days at 4 °C. After washing in PBS, specimens were immersed in PBS containing 30% sucrose for cryoprotection. The tissue was embedded in O.C.T. compound (Miles, Elkhart, IN, USA), cryosectioned (10–20 μm in thickness) serially in vertical direction on a cryostat (Leica, Nussloch, Germany) at −20 °C, and mounted on gelatin-coated slides. After dried at −20 °C or −80 °C, cryosections were observed for rhodamine-labeling of Neurobiotin-localization. The sections were incubated in a blocking solution of 20% normal goat serum in PBS to block nonspecific binding. The sections were then incubated with rabbit anti-GABA antibody (glutaraldehyde-conjugated polyclonal antibody, Chemicon, Temecula, CA), diluted with 1:500, for overnight at 4 °C. After washing, the sections were incubated with FITC-conjugated secondary antibody (MBL, Nagoya, Japan).

For connexins identification of gap junctions between goldfish amacrine cells, the retinas involving LY-filled cells (see above) were fixed with the paraformaldehyde fixative following electrophysiological identification of amacrine cells (see above). The tissue was then incubated with the primary and secondary antibodies according to Hidaka et al. (2004). The tissue was incubated with the anti-Cx36 antibody, diluted 1: 250 with PBS (Hidaka et al., 2004) or monoclonal mouse antibody to perch Cx35 (anti-Cx35/36; clone 8 F6.2; MAB3045, Millipore Bioscience Research Reagents, Billerica, MA), diluted 1:500 (Li et al., 2009). The tissue was also examined with monoclonal anti-Cx26 (diluted 1:500, Zymed, South San Francisco, CA), anti-Cx32 (diluted 1:500, Zymed) and anti-Cx43 antibody (diluted 1 : 500, Chemicon). The specimens were then incubated in goat anti-rabbit IgG (H+L), conjugated with Alexa Fluor 546 (absorption 556 nm/max emission 575 nm, Molecular Probes, Eugene, OR).

The immunolabeled specimens were examined under an epifluorescence microscope with a blue excitation for the FITC or Alexa Fluor 488 fluorescent labeling, and a green excitation (Nikon, Tokyo, Japan) for the rhodamine or Alexa Fluor 546 labeling. Fluorescent images were also taken on confocal laser-scanning microscopes (Carl Zeiss LSM310 or LSM510, Germany), using the Multi-Scan function with a combination of the 543 nm laser under the 560 nm cut filter for rhodamine labeling of amacrine cells or immunofluorescence of connexin, and the 458 nm line of an argon laser under a band pass filter of 475–545 nm for LY labeling of amacrine cells or the 488 nm laser under a band pass filter of 500–530 nm for GABA-labeling probed by FITC or Alexa Fluor 488. Digital images acquired from the confocal microscope were processed in Adobe Photoshop (Adobe System, Inc.; San Jose, CA) to adjust brightness and color contrast of the multichannel signals.

5.7. *Electron microscopic analysis*

According to methods previously described for three-dimensional analysis of dendrodendritic connections between Neurobiotin-labeled amacrine cells by high-voltage electron microscopy (Hidaka et al., 1986, 1993, 2004, 2005), the DAB visualization was performed by the heavy metal intensification of horseradish peroxidase (HRP) reaction in the presence of 0.1 M $(NH_4)_2Ni(SO_4)_2$ and 0.1 M $CoCl_2$, dissolved in 0.1 M Tris buffer, pH 7.8 (see Adams, 1981). The reaction products were further processed by the photochromic intensification with 0.02% nitro blue tetrazolium (Sigma), dissolved in 0.1 M Tris buffer, pH 8.2, under green excitation of fluorescent microscopy (see Vaney, 1992). Prior to electron microscopical analysis of dendrodendritic connections between the cells, the specimens were examined light-microscopically.

For ultrastructural examination of connections between amacrine cells, tissues were postfixed in 1% OsO_4 in PBS, dehydrated in a series of ethanol-water mixtures, and embedded in a mixture of Epoxy resins involving Glycidether 100 (Serva, Heidelberg, Germany). To enhance electron density of the specimens for high-voltage electron microscopical analysis of thick sections, en bloc stainings were made in three steps of 3% $K_2Cr_2O_7$ in D.W., 2% uranyl acetate in 70% ethanol, and 20% phosphotungstic acid in the absolute ethanol. Serial tangential sections (5 μm in thickness) of the cells to be studied were made (see Hidaka et al., 1986, 2004, 2005), and the material was examined in a HITACHI H-1250 M high-voltage electron microscope at 1000 kV (National Institute for Physiological Sciences, Okazaki, Japan). For analysis of junctional structures between the interconnected dendrites of amacrine cells, serial ultrathin sections from the specimens were studied in a JEM 1010, JEOL 1200EX or HITACHI H-7650, H-7000 conventional electron microscope at 75 kV or 80 kV fitted with a goniometer stage.

Acknowledgments

This work was performed in the 21st-Century COE Program to Fujita Health University (Directors: Drs. Yoshizo Asano and Yoshikazu Kurosawa) from the Japanese Ministry of Education, Culture, Sports, Science and Technology. Our studies were in part supported by the Science Research Promotion Fund from the Promotion and Mutual Aid Corporation for Private Schools of Japan (No. 231016), and by Grants-in-Aid for Scientific Research from the Japanese Ministry of Education, Culture, Sports, Science and Technology to S.H. (No. 03857020, 04857016 and 10680754). I am grateful to Dr. Roman R. Poznanski for reading the first draft of this manuscript, and providing helpful suggestions for improvement. My high-voltage electron microscopical studies were performed in the co-operative program of National Institute for Physiological Sciences (Okazaki) with numbers of 2008-HVEM06, 2009-HVEM502, 2010-HVEM516 and 2011-HVEM506. I greatly appreciate Drs. Kazuyoshi Murata, Tatsuo Arii, Noboru Yamaguchi and Katsumi Kato for excellent maintenance of the HITACHI H-1250M electron microscope and valuable advice pertaining to ultrastructural studies. I thank Drs. Gen Niini, Toshiaki Kato, Yang Lu and Yoko Hashimoto for technical advice pertaining to ultrastructural and histochemical experiments, and Chieko Nishikawa, Masayo Kamiya, Michiyo Maehara, Keiichi Iizuka, Daisuke Ishihara, Junko Ikoma and Mayu Watanabe for technical assistance.

REFERENCES

Adams, J.C., 1981. Heavy metal intensification of DAB-based HRP reaction product. J. Histochem. Cytochem. 29, 775.

Baylor, D.A., Hodgkin, A.L., Lamb, T.D., 1974. The electrical response of turtle cones to flashes and steps of light. J. Physiol. 242, 685–727.

Bennett, M.V.L., Barrio, L.C., Bargiello, T.A., Spay, D.C., Hertzberg, E., Saez, J.C., 1991. Gap junctions: new tools, new answers, new questions. Neuron 6, 305–317.
Bloomfield, S.A., Völgyi, B., 2004. Function and plasticity of homologous coupling between AII amacrine cells. Vision Res. 44, 3297–3306.
Bloomfield, S.A., Völgyi, B., 2009. The diverse functional roles and regulation of neuronal gap junctions in the retina. Nat. Rev. Neurosci. 10, 495–506.
Bruzzone, R., White, T.W., Paul, D.L., 1996. Connections with connexins: the molecular basis of direct intercellular signaling. Eur. J. Biochem. 238, 1–27.
Chino, Y., Hashimoto, Y., 1986. Dopaminergic amacrine cells in the retina of Japanese dace. Brain Res. 372, 323–337.
Dacheux, R.F., Raviola, E., 1986. The rod pathway in the rabbit retina: a depolarizing bipolar and amacrine cell. J. Neurosci. 6, 331–345.
DeVries, S.H., Schwartz, E.A., 1989. Modulation of an electrical synapse between solitary pairs of catfish horizontal cells by dopamine and second messengers. J. Physiol. (Lond.) 414, 351–375.
Djamgoz, M.B.A., Downing, J.E.G., Wager, H.-J., 1989. Amacrine cells in the retina of a cyprinid fish: functional characterization and intracellular labelling with horseradish peroxidase. Cell Tissue Res. 256, 607–622.
Djamgoz, M.B.A., Spadavecchia, L., Usai, C., Vallerga, S., 1990. Variability of light-evoked response pattern and morphological characterization of amacrine cells in goldfish retina. J. Comp. Neurol. 301, 171–190.
Djupsund, K., Furukawa, T., Yasui, S., Yamada, M., 2003. Asymmetric temporal properties in the receptive field of retinal transient amacrine cells. J. Gen. Physiol. 122 (4), 445–458.
Dowling, J.E., 1987. The Retina: An Approachable Part of the Brain. Harvard University Press, Massachusetts.
Dunn, F.A., Doan, T., Sampath, A.P., Rieke, F., 2006. Controlling the gain of rod-mediated signals in the mammalian retina. J. Neurosci. 26, 3959–3970.
Famiglietti, E.V., Kaneko, A., Tachibana, M., 1977. Neuronal architecture of ON and OFF pathways to ganglion cells in carp retina. Science 198, 1267–1269.
Fried, S.I., Masland, R.H., 2007. Image processing: how the retina detects the direction of image motion. Curr. Biol. 17 (2), R63–R66.
Goodenough, D.A., Goliger, J.A., Paul, D.L., 1996. Connexins, connexons, and intercellular communication. Annu. Rev. Biochem. 65, 75–502.
Hampson, E.C.G.M., Vaney, D.I., Weiler, R., 1992. Dopaminergic modulation of gap junction permeability between amacrine cells in mammalian retina. J. Neurosci. 12 (12), 4911–4922.
Hashimoto, Y., Kato, A., Inokuchi, M., Watanabe, K., 1976. Re-examination of horizontal cells in the carp retina with procion yellow electrode. Vision Res. 16 (1), 25–29.
Hidaka, S., 2008. Intracellular cyclic-AMP suppresses the permeability of gap junctions between retinal amacrine cells. J. Integr. Neurosci. 7 (1), 29–48.
Hidaka, S., Ishida, A.T., 1998. Voltage-gated Na^+ current availability after step- and spike-shaped conditioning depolarizations of retinal ganglion cells. Pflügers Arch. 436, 497–508.
Hidaka, S., Christensen, B.N., Naka, K., 1986. The synaptic ultrastructure in the outer plexiform layer of the catfish retina: a three-dimensional study with HVEM and conventional EM of Golgi-impregnated bipolar and horizontal cells. J. Comp. Neurol. 247, 181–199.
Hidaka, S., Shingai, R., Dowling, J.E., Naka, K., 1989. Junctions form between catfish horizontal cells in culture. Brain Res. 498, 53–63.
Hidaka, S., Maehara, M., Umino, O., Lu, Y., Hashimoto, Y., 1993. Lateral gap junction connections between retinal amacrine cells summating sustained responses. Neuroreport 5, 29–32.
Hidaka, S., Akahori, Y., Kurosawa, Y., 2004. Dendrodendritic electrical synapses between mammalian retinal ganglion cells. J. Neurosci. 24 (46), 10553–10567.
Hidaka, S., Kato, T., Hashimoto, Y., 2005. Structural and functional properties of homologous electrical synapses between retinal amacrine cells. J. Integr. Neurosci. 4 (3), 313–340.
Kaneko, A., 1970. Physiological and morphological identification of horizontal, bipolar, and amacrine cells in goldfish retina. J. Physiol. (Lond.) 207, 623–633.
Kaneko, A., 1973. Receptive field organization of bipolar and amacrine cells in the goldfish retina. J. Physiol. (Lond.) 235, 133–153.
Kebabian, J.W., Calne, D.B., 1979. Multiple receptors for dopamine. Nature 277, 193–196.
Kolb, H., Nelsen, R., 1983. Rod pathways in the retina of the cat. Vision Res. 23, 301–312.
Kothmann, W.W., Massey, S.C., O'Brien, J., 2009. Dopamine-stimulated dephosphorylation of connexin 36 mediates AII amacrine cell uncoupling. J. Neurosci. 29 (47), 14903–14911.
Lasater, E., 1987. Retinal horizontal cell gap junctional conductance is modulated by dopamine through a cyclic AMP-dependent protein kinase. Proc. Natl. Acad. Sci. USA 84, 7319–7323.
Lasater, E.M., Dowling, J.E., 1985. Dopamine decreases conductance of the electrical junctions between cultured retinal horizontal cells. Proc. Natl. Acad. Sci. USA 82, 3025–3029.
Li, H., Chuang, A.Z., O'Brien, J., 2009. Photoreceptor coupling is controlled by connexin 35 phosphorylation in zebrafish retina. J. Neurosci. 29 (48), 15178–15186.
Marc, R.E., Stell, W.K., Bok, D., Lam, D.M., 1978. GABA-ergic pathways in the goldfish retina. J. Comp. Neurol. 182 (2), 221–244.
Marc, R.E., Liu, W.L., Muller, J.F., 1988. Gap junctions in the inner plexiform layer of the goldfish retina. Vision Res. 28 (1), 9–24.
Masland, R.H., 2001. The fundamental plan of the retina. Nat. Neurosci. 4, 877–885.
Masland, R.H., 2005. The many roles of starburst amacrine cells. Trends Neurosci. 28 (8), 395–396.
Mastronarde, D.N., 1983. Correlated firma of cat retinal aanalion cells. II. Responses of X- and Y-cells to single quanta1 events. J. Neurophysiol. 49, 325–349.
Mastronarde, D.N., 1989. Correlated firing of cat retinal ganglion cells. Trends Neurosci. 12, 75–80.
McMahon, D.G., Knapp, A.G., Dowling, J.E., 1989. Horizontal cell gap junctions: single-channel conductance and modulation by dopamine. Proc. Natl. Acad. Sci. USA 86, 7639–7643.
Meister, M., Lagnado, L., Baylor, D.A., 1995. Concerted signaling by retinal ganglion cells. Science 270, 1207–1210.
Naka, K., Christensen, B.N., 1981. Direct electrical connections between transient amacrine cells in the catfish retina. Science 214, 462–464.
Negishi, K., Teranishi, T., 1990. Close tip to tip contacts between dendrites of transient amacrine cells in carp retina. Neurosci. Lett. 115, 1–6.
Negishi, K., Teranishi, T., Kato, S., 1985. Opposite effects of ammonia and carbon dioxide on dye coupling between horizontal cells in the carp retina. Brain Res. 342 (2), 330–339.
Nelson, R., 1982. AI1 amacrine cells quicken time course of rod signals in the cat retina. J. Neurophysiol. 47, 928–947.
Neve, K.A., Seamans, J.K., Trantham-Davidson, H., 2004. Dopamine receptor signaling. J. Recept. Signal Transduct. Res. 24 (3), 165–205.
Pan, F., Mills, S.L., Massey, S.C., 2007. Screening of gap junction antagonists on dye coupling in the rabbit retina. Vis. Neurosci. 24, 609–618.
Penn, A.A., Wong, R.O.L., Shatz, C.L., 1994. Neuronal coupling in the developing mammalian retina. J. Neurosci. 14, 3805–3815.
Piccolino, M., Neyton, J., Gerschenfeld, H.M., 1984. Decrease of gap junction permeability induced by dopamine and cyclic adenosine 3′: 5′-monophosphate in horizontal cells of turtle retina. J. Neurosci. 4, 2447–2488.
Poznanski, R.R., 2005. Biophysical mechanisms and essential topography of directionally selective subunits in rabbit's retina. J. Integr. Neurosci. 4 (3), 341–361.

Poznanski, R.R., 2010a. Analytical solution of reaction–diffusion equations for calcium wave propagation in a starburst amacrine cell. J. Integr. Neurosci. 9 (3), 283–297.
Poznanski, R.R., 2010b. Cellular inhibitory behavior underlying the formation of retinal direction selectivity in the starburst network. J. Integr. Neurosci. 9 (3), 299–335.
Poznanski, R.R., Umino, O., 1997. Syncytial integration by a network of coupled bipolar cells in the retina. Prog. Neurobiol. 53, 273–291.
Sakai, H.M., Naka, K., 1992. Response dynamics and receptive-field organization of catfish amacrine cells. J. Neurophysiol. 67, 430–442.
Sakai, H.M., Machuca, H., Naka, K., 1997. Processing of color- and noncolor-coded signals in the gourami retina. II. amacrine cells. J. Neurophysiol. 78, 2018–2033.
Sakmann, B., Neher, E., 1995. Single-channel Recording, 2nd edn. Plenum Press, N.Y.
Schorderet, M., 1989. Receptors coupled to adenylate cyclase in isolated rabbit retina. Neurochem. Int. 14, 387–395.
Shimoda, Y., Hidaka, S., Maehara, M., Lu, Y., Hashimoto, Y., 1992. Hyperpolarizing interplexiform cell of the dace retina identified physiologically and morphologically. Vis. Neurosci. 8 (3), 193–199.
Söhl, G., Maxeiner, S., Willecke, K., 2005. Expression and functions of neuronal gap junctions. Nat. Rev. Neurosci. 6 (3), 191–200.
Stell, W.K., Lightfood, D.O., Wheeler, T.G., Leeper, H.F., 1975. Goldfish retina: functional polarization of cone horizontal cell dendrites and synapses. Science 190, 989–990.
Tauchi, M., Masland, R.H., 1984. The shape and arrangement of the cholinergic neurons in the rabbit retina. Proc. R. Soc. Lond. B Biol. Sci. 223, 101–119.
Taylor, W.R., Vaney, D.I., 2003. New directions in retinal research. Trends Neurosci. 26 (7), 379–385.
Teranishi, T., Negishi, K., 1991. Dendritic morphology of a class of interstitial and normally placed amacrine cells revealed by intracellular Lucifer yellow injection in carp retina. Vision Res. 31 (3), 463–475.
Teranishi, T., Negishi, K., 1994. Double-staining of horizontal and amacrine cells by intracellular injection with lucifer yellow and biocytin in carp retina. Neuroscience 59, 217–226.
Teranishi, T., Negishi, K., Kato, S., 1983. Dopamine modulates S-potential amplitude and dye-coupling between external horizontal cells in carp retina. Nature 301, 243–246.
Teranishi, T., Negishi, K., Kato, S., 1984. Regulatory effect of dopamine on spatial properties of horizontal cells in carp retina. J. Neurosci. 4, 1271–1286.
Teranishi, T., Negishi, K., Kato, S., 1987. Correlations between photoresponse and morphology of amacrine cells in the carp retina. Neuroscience 20, 935–950.
Umino, O., Maehara, M., Hidaka, S., Kita, K., Hashimoto, Y., 1994. The network properties of bipolar–bipolar coupling in the retina of teleost fishes. Vis. Neurosci. 11, 533–548.
Van Buskirk, R., Dowling, J.E., 1981. Isolated horizontal cells from carp retina demonstrate dopamine-dependent accumulation of cyclic AMP. Proc. Natl. Acad. Sci. USA 78, 7825–7829.
Vaney, D.I., 1991. Many diverse types of retinal neurons show tracer coupling when injected with biocytin or Neurobiotin. Neurosci. Lett. 125, 187–190.
Vaney, D.I., 1992. Photochromic intensification of diaminobenzidine reaction product in the presence of tetrazolium salts: applications for intracellular labelling and immunohistochemistry. J. Neurosci.Methods 44, 217–223.
Vaney, D.I., 1994. Patterns of neuronal coupling in the retina. In: Osborne, N.N., Chader, G.J. (Eds.), Prog. Retinal Eye Res., Vol. 13. Pergamon Press, Oxford, pp. 301–355.
Vaney, D.I., Taylor, W.R., 2002. Direction selectivity in the retina. Curr. Opin. Neurobiol. 12 (4), 405–410.
Vardi, N., Smith, R.G., 1996. The AII amacrine network: coupling can increase correlated activity. Vision Res. 36, 3743–3757.
Veruki, M.L., Hartveit, E., 2009. Meclofenamic acid blocks electrical synapses of retinal AII amacrine and ON-cone bipolar cells. J. Neurophysiol. 101, 2339–2347.
Wagner, H.-J., Wagner, E., 1988. Amacrine cells in the retina of a teleost fish, the roach (*Rutilus rutilus*): a Golgi study on differentiation and layering. Philos. Trans. R. Soc. Lond. Biol. 321, 263–324.
Watling, K.J., Dowling, J.E., Iversen, L.L., 1979. Donamine receptors in the retina may all-be linked to adenylate cyclase. Nature 281, 578–580.
White, T.W., Paul, D.L., 1999. Genetic diseases and gene knockouts reveal diverse connexin functions. Annu. Rev. Physiol. 61, 283–310.
Yang, C.Y., Lukasiewicz, P., Maguire, G., Werblin, F.S., Yazulla, S., 1991. Amacrine cells in the tiger salamander retina: morphology, physiology, and neurotransmitter identification. J. Comp. Neurol. 312 (1), 19–32.

Glossary

ABC: avidin–biotin–HRP complex
cAMP: adenosine 3′,5′-cyclic monophosphate
cGMP: guanosine 3′,5′-cyclic monophosphate
Cx: connexin
DAB: diaminobenzidine
FITC: fluorescein 5(6)-isothiocyanate
Gj: electrical junction conductance
GABA: γ-aminobutyric acid
GCL: ganglion cell layer
HRP: horseradish peroxidase
INL: inner nuclear layer
IPL: inner plexiform layer
ISAC: interstitial amacrine cell
LY: Lucifer Yellow
OPL: outer plexiform layer
PBS: phosphate buffer saline
s-a: sublamina-a of the IPL
s-b: sublamina-b of the IPL
TBS: Tris-buffered saline
8-br-cAMP: 8-bromoadenosine 3′,5′-cyclic monophosphate